

Radiolabeled Interleukin-8: Specific Scintigraphic Detection of Infection Within a Few Hours

Conny J. van der Laken, Otto C. Boerman, Wim J.G. Oyen, Marjo T.P. van de Ven, Jos W.M. van der Meer, and Frans H.M. Corstens

Departments of Nuclear Medicine and Internal Medicine, University Hospital Nijmegen, Nijmegen, The Netherlands

Several small receptor-binding agents have been tested for imaging of infection and inflammation. The potential of chemotactic peptides and of interleukins is promising and superior to that of conventional agents. In this study, we investigated the potential of interleukin-8 (IL-8) to image infection in rabbits. **Methods:** IL-8 was labeled with ^{123}I using the Bolton-Hunter method. Twenty-four hours after induction of *Escherichia coli* abscesses in the left thigh muscle, rabbits were injected intravenously with 18.5 MBq ^{123}I -IL-8. γ Camera images were obtained at 5 min and at 1, 4, and 8 h after injection. Biodistribution was determined 8 h after injection. **Results:** ^{123}I -IL-8 rapidly cleared from the blood. Accumulation of ^{123}I -IL-8 in the abscess was visible as early as 1 h after injection. The highest abscess uptake was obtained 4 h after injection (2.6 ± 0.2 percentage injected dose [%ID]), whereas ^{123}I -IL-8 rapidly cleared from all other tissues. This resulted in increases in abscess-to-background ratios to 13.0 ± 0.7 (8 h after injection), as determined by quantification of the images. In tissue biodistribution (8 h after injection), the abscess uptake was 0.057 ± 0.011 %ID/g with abscess-to-contralateral muscle ratios of 114.7 ± 23.0 . The radioiodination method clearly affected the in vivo biodistribution of IL-8 because IL-8 iodinated using the Iodo-Gen method cleared significantly slower from the blood and most other organs, resulting in poor visualization of the abscess. **Conclusion:** The superior characteristics of IL-8 radiiodinated using the Bolton-Hunter method—i.e., high abscess uptake and rapid background clearance within a few hours—make IL-8 a promising agent to image infection and inflammation.

Key Words: interleukin-8; infection; imaging; biodistribution; Bolton-Hunter

J Nucl Med 2000; 41:463–469

Timely identification of the localization and extent of infectious and inflammatory foci is crucial to enable adequate treatment of patients with infectious or inflammatory diseases. Conventional scintigraphic techniques using ^{67}Ga -citrate, labeled leukocytes, or immunoglobulin G (IgG) (1–3) are appropriate for detection of infection and sterile inflammation, but at least 12–24 h are required before a

diagnosis can be established. Agents providing a same-day answer would therefore be highly desirable.

Small receptor-binding agents have been proposed to obtain high specific uptake at the site of infection or inflammation within several hours after injection. The potential of such agents—i.e., chemotactic peptides and interleukins—to image infection and inflammation has been evaluated by several investigators. Accumulation of $^{99\text{m}}\text{Tc}$ -labeled chemotactic peptides in focal infections in rabbits appeared to be superior to both ^{111}In -labeled IgG (4) and ^{111}In -labeled white blood cells (WBCs) (5). Specific retention in several focal infections and sterile inflammations was also obtained with radioiodinated interleukin-1 (IL-1) in mice, characterized by high target-to-background ratios (6,7). Furthermore, lymphocytic infiltration has been visualized successfully with radiolabeled interleukin-2 in patients with thyroiditis (8).

Interleukin-8 (IL-8) is another interleukin that may be suitable for scintigraphic detection of infection and inflammation. This small protein (10 kDa) belongs to the CXC subfamily of the chemokines, in which the first 2 cysteines are separated by 1 amino acid. Chemokines or chemotactic cytokines are involved in cell activation and recruitment of cells to the area of inflammation. The CXC chemokines play an important role in cell recruitment during acute inflammation (9). IL-8 induces chemotaxis of neutrophils (10). High concentrations of IL-8 have been observed in various inflammatory conditions and correlate with tissue neutrophil infiltration in diseases such as rheumatoid arthritis (11), adult respiratory distress syndrome (12), and ulcerative colitis (13,14). Neutrophils express 2 types of IL-8 receptors (15,16). IL-8 binds to both receptors with high affinity (0.3–4 nmol/L) (17,18).

Therefore, on theoretic grounds, systemically administered radiolabeled IL-8 may target inflammatory tissue, where massive infiltration of neutrophils is present, by specific receptor binding to these cells. In this study, we investigated the potential of radioiodinated IL-8 for imaging infection in a rabbit model.

MATERIALS AND METHODS

Radioiodination

Human recombinant IL-8 was kindly provided by Dr. Ivan Lindley (Novartis, Vienna, Austria). IL-8 was radiolabeled with ^{123}I

Received Oct. 25, 1998; revision accepted Apr. 19, 1999.

For correspondence or reprints contact: Otto C. Boerman, PhD, Department of Nuclear Medicine, University Hospital Nijmegen, P.O. Box 9101, 6500 HB Nijmegen, The Netherlands.

using the Bolton-Hunter method (19). Briefly, in each of 4 vials, 2.5 μ g Bolton-Hunter reagent (Pierce Chemical Co., Rockford, IL) was radiolabeled with 150 MBq Na¹²³I (Cygne, Eindhoven, The Netherlands; specific activity, 2×10^{17} Bq/mol) by incubating it with 5 μ g N-chlorosuccinimide during 10 min at room temperature in methanol. The reaction was terminated by adding 5 μ g Na₂S₂O₅ to the reaction mixture. The methanol was evaporated with a gentle stream of N₂. Subsequently, 50 μ g IL-8 in 2 μ L 1.0 mol/L bicarbonate buffer, pH 8.2, was added per vial and incubated for 30 min on ice.

To study the effect of the radioiodination method on the in vivo biodistribution of ¹²³I-IL-8, IL-8 was also labeled according to the Iodo-Gen (1,3,4,6-tetrachloro-3 α ,6 α -diphenylglycoluril; Pierce) method (20). Briefly, 200 μ g IL-8, 75 MBq Na¹²³I, and 100 mmol/L phosphate buffer, pH 7.2 (total volume, 100 μ L), were added to glass tubes, precoated with Iodo-Gen (10 μ g/100 μ L). The reaction was allowed to proceed for 10 min at room temperature.

After the labeling reaction, the reaction mixtures were pooled and applied to a Sephadex G-25 column (PD-10; Pharmacia, Uppsala, Sweden) and eluted with 0.25% gelatin in phosphate-buffered saline to separate labeled agents from unconjugated ¹²³I. The void fractions were pooled and sterilized through a 0.2- μ m filter (Millipore, Inc., Milford, MA).

The radiochemical purity of the radiopharmaceuticals was determined by instant thin-layer chromatography (ITLC) on ITLC-SG strips (Gelman Laboratories, Ann Arbor, MI) with 0.1 mol/L citrate, pH 5.0, as the mobile phase. In addition, all radiolabeled IL-8 preparations were analyzed by high-performance liquid chromatography (HPLC) on a Biologic HR system (Bio Rad Labs, Hercules, CA), using a Shodex KW-802.5 size-exclusion column (molecular weight range, 100–50,000 Da) (Millipore), eluted with a mixture of Tris-HCl and 0.025% gelatin, pH 7.4, at a flow rate of 0.5 mL/min.

In this article, ¹²³I-IL-8 refers to IL-8 radiolabeled using the Bolton-Hunter method unless stated otherwise.

Receptor-Binding Assay

Heparinized human whole blood (10 mL) was mixed with 2.5 mL 5% dextran (Sigma, St. Louis, MO). After red blood cell sedimentation during 1 h at room temperature, the blood free of red blood cells was washed in incubation buffer (1 mmol/L NaH₂PO₄, 5 mmol/L Na₂HPO₄, 140 mmol/L NaCl, 0.5 mmol/L MgCl₂, and 0.15 mmol/L CaCl₂, pH 7.4) and centrifuged at 500g for 20 min. The cell pellet was then resuspended in 7 mL incubation buffer and layered on 5 mL Ficoll-Hypaque (Pharmacia) followed by centrifugation at 500g for 20 min. Contaminating erythrocytes were removed from the pellet, rich with polymorphonuclear cells (PMNs), by hypotonic lysis. The PMN pellet was washed once and subsequently resuspended in incubation buffer supplemented with 0.5% bovine serum albumin. A series of serially diluted PMN suspensions ($0.5\text{--}8 \times 10^6$ PMNs/mL) was incubated with 10,000 cpm of radioiodinated IL-8. A duplicate of the lowest cell concentration was incubated in the presence of a 100-fold molar excess of unlabeled IL-8 to correct for nonspecific binding. After 2 h of incubation at 4°C, PMNs were centrifuged (5 min, 2000g), and the radioactivity in the pellet (total bound activity) was measured in a shielded well scintillation γ counter (Wizard; Pharmacia-LKB, Uppsala, Sweden). The data were graphically analyzed in a modified Lineweaver-Burk plot: a double inverse plot of the conventional binding plot (specifically bound fraction versus cell concentration) (21). The receptor-binding fraction at infinite cell excess was calculated by linear extrapolation to the ordinate.

Animal Studies

Abscesses were induced in the left thigh muscle of female New Zealand white rabbits weighing 2.2–2.8 kg with 1.5×10^{10} colony-forming units of *Escherichia coli* in 0.5 mL. During the procedure, rabbits were anesthetized with a subcutaneous injection of a 0.6-mL mixture of fentanyl (0.315 mg/mL) and fluanisone (10 mg/mL) (Hypnorm; Janssen Pharmaceutical, Buckinghamshire, UK). After 24 h, when swelling of the muscle was apparent, groups of at least 3 rabbits ($n = 6$ for ¹²³I-IL-8 labeled using the Bolton-Hunter method; $n = 3$ for ¹²³I-IL-8 labeled using the Iodo-Gen method) were immobilized, placed prone on the γ camera, and injected with 18.5 MBq of 65 μ g ¹²³I-IL-8 in the lateral ear vein.

Images were recorded at 5 min and at 1, 4, and 8 h after injection with a single-head γ camera (Orbiter; Siemens Medical Systems, Hoffman Estates, IL) equipped with a parallel-hole, medium-energy collimator. Images were obtained with a 15% symmetric window over the 158-keV ¹²³I energy peak. After acquisition of 50,000–100,000 counts, the images were digitally stored in a 256×256 matrix.

Scintigraphic images were analyzed quantitatively by drawing regions of interest (ROIs) over the heart, lungs, abscess, uninfected contralateral thigh muscle (background), and whole body. The uptake of activity in the various tissues was subsequently determined by measurement of the activity in the ROIs. The uptake in the ROIs was expressed as percentage of the total body activity at 5 min after injection (%ID), which was set as 100%. Abscess-to-background ratios were calculated.

After obtaining of the final images, rabbits were killed with a lethal dose of sodium phenobarbital. Samples of blood, infected thigh muscle, uninfected contralateral thigh muscle, bone, bone marrow, lung, spleen, liver, kidneys, and intestines were collected. The dissected tissues were weighed, and the radioactivity was counted in the γ counter. To correct for radioactive decay, injection standards were counted simultaneously. The measured activity in samples was expressed as percentage of injected dose per gram tissue (%ID/g). Abscess-to-contralateral muscle ratios and abscess-to-blood ratios were calculated.

The blood clearance of both ¹²³I-IL-8 preparations was determined in rabbits with intramuscular *E. coli* infections (3 rabbits per radiolabeled preparation). Blood samples were collected at 1, 5, 10, 20, 30, 60, 120, and 240 min after injection of the radiopharmaceuticals. Blood samples were weighed, their activity was measured, and their uptake was expressed as %ID/g.

In addition, WBC counts were measured in blood samples of healthy rabbits after injection of an equal amount of ¹²³I-IL-8 as that used in imaging and biodistribution studies. Blood samples were obtained at 1, 3, 5, 10, 30, and 60 min after injection.

Statistical Analysis

All values are expressed as mean \pm SEM. The data were analyzed statistically using the 1-way ANOVA.

RESULTS

Radiolodination and Characterization of ¹²³I-IL-8

The labeling efficiency of the radioiodination of IL-8 using the Bolton-Hunter method was between 25% and 35%. On average, 1 Bolton-Hunter molecule was conjugated to 1 IL-8 molecule. In the case of the Iodo-Gen method, the labeling efficiency was 60%–80%. The specific activity of all ¹²³I-IL-8 preparations was 0.2–0.6 MBq/ μ g.

The radiochemical purity of all radiopharmaceuticals was greater than 95% after gel filtration (Fig. 1).

The receptor-binding capacity of all ^{123}I -IL-8 preparations, regardless of the labeling method, was preserved after radioiodination: The receptor-binding fraction for conditions representing infinite cell receptor excess was always between 50% and 75% (Fig. 2).

^{123}I -IL-8 in Rabbits with *E. coli* Infection

Immediately after injection of ^{123}I -IL-8 in healthy rabbits, a transient reduction of peripheral leukocyte levels to 45% was observed (Fig. 3). The WBC count returned to 90%–95% within 10 min after injection, followed by an increase to 170%, which was still present 1 h after injection.

During the first 10 min after injection, ^{123}I -IL-8, labeled using the Bolton-Hunter method, rapidly cleared from the blood with a $t_{1/2} < 5$ min (Fig. 4A). After 10 min, no further decrease of ^{123}I -IL-8 blood levels was observed until 30 min. Thereafter, ^{123}I -IL-8 cleared with a $t_{1/2}$ of 80.8 ± 3.3 min. These 3 phases of clearance were also observed with ^{123}I -IL-8, labeled using the Iodo-Gen method (Fig. 4B).

The images showed clear delineation of the abscesses as early as 1 h after injection (Fig. 5). Immediately after injection, uptake of ^{123}I -IL-8 was also observed in the lungs and slowly decreased during the first 4 h. In addition, activity was found in the kidneys and bladder.

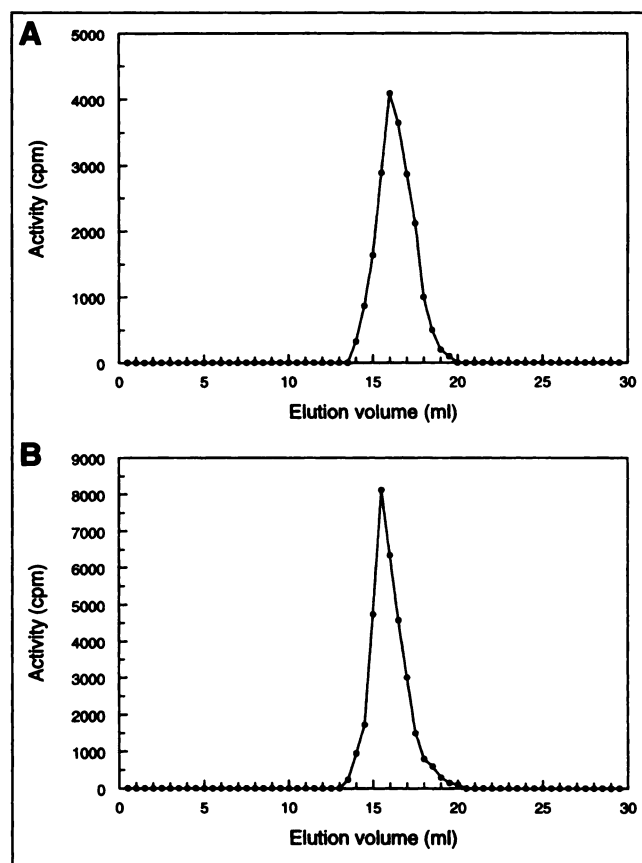


FIGURE 1. HPLC elution profiles of ^{123}I -BH-IL-8 (A) and ^{123}I -Iod-IL-8 (B) preparations before injection.

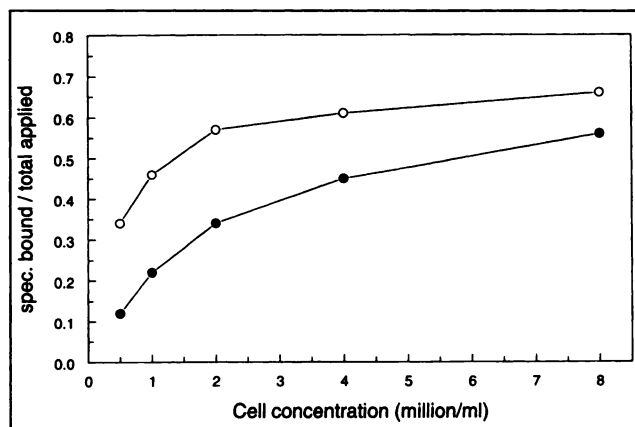


FIGURE 2. Binding plots of ^{123}I -BH-IL-8 (●) and ^{123}I -Iod-IL-8 (○) determined on isolated human granulocytes. Specifically bound fraction is plotted as function of increasing cell concentration.

After injection, ^{123}I -IL-8 rapidly accumulated at the site of infection. The peak value in the abscess of 2.6 ± 0.2 %ID was found at 4 h after injection (Fig. 6A). The absolute uptake in the abscess decreased thereafter to $1.5\% \pm 0.2\%$ at 8 h after injection, as assessed by quantitative analysis of the images. Because of the rapid background clearance, the abscess-to-background ratios increased continuously from 1.3 ± 0.04 at 5 min after injection to 13.0 ± 0.7 at 8 h after injection (Fig. 6B). Tissue biodistribution determined at 8 h after injection showed that, except for the kidneys, the highest uptake of ^{123}I -IL-8 was found in the abscess—i.e., 0.057 ± 0.011 %ID/g (Table 1). The abscess-to-contralateral muscle ratios reached a value as high as 114.7 ± 23.0 at 8 h after injection. The abscess-to-blood ratio was 12.1 ± 2.2 at 8 h after injection.

Effect of Labeling Method on Biodistribution of ^{123}I -IL-8

The radioiodination method clearly affected the biodistribution of ^{123}I -IL-8 (Table 1). ^{123}I -IL-8 labeled using the Iodo-Gen method (^{123}I -Iod-IL-8) cleared slower than when

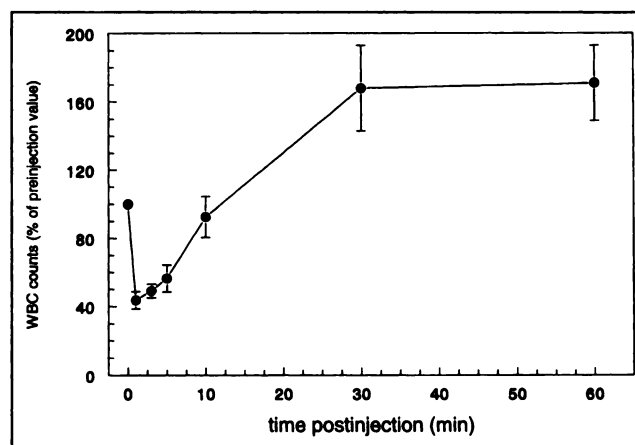


FIGURE 3. WBC counts in blood of healthy New Zealand white rabbits after intravenous injection of $65 \mu\text{g}$ ^{123}I -IL-8 expressed as percentage of preinjection value.

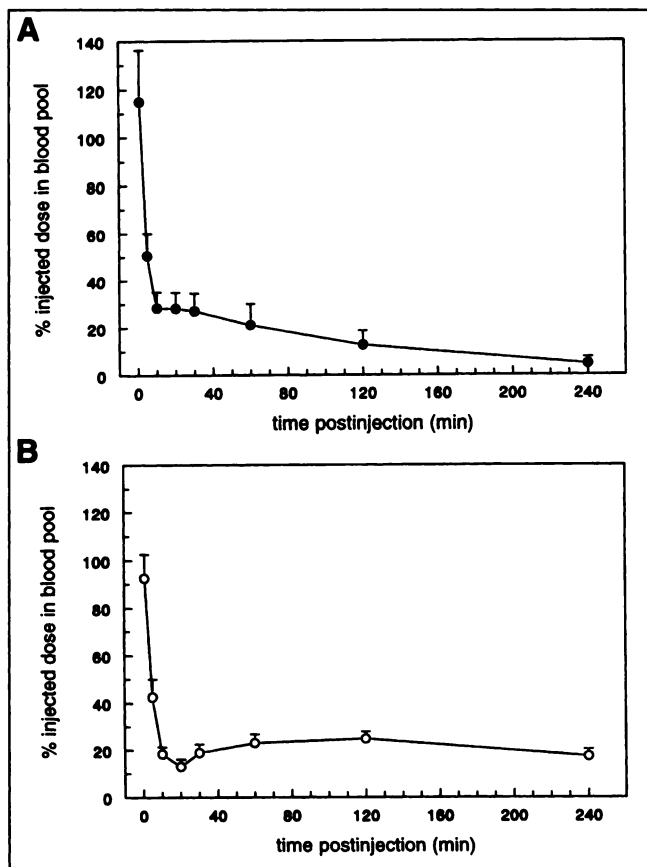


FIGURE 4. Blood clearance of ^{123}I -BH-IL-8 (A) and ^{123}I -iod-IL-8 (B) determined in rabbits with *E. coli* infection. Data are expressed as percentage of injected dose in blood pool. Error bars indicate SEM.

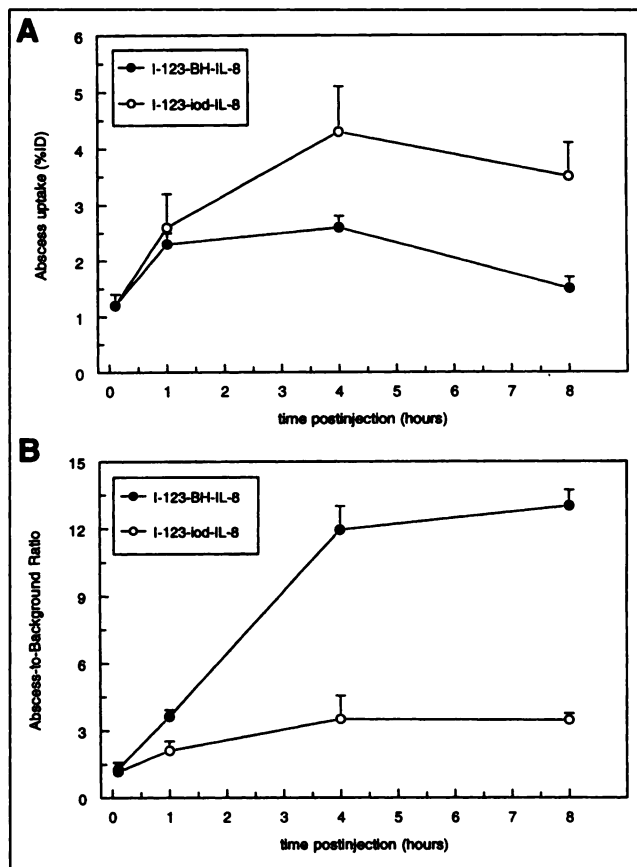


FIGURE 6. (A) Abscess uptake determined by quantitative analysis of images of rabbits with *E. coli* infection injected with ^{123}I -BH-IL-8 (●) or ^{123}I -iod-IL-8 (○). Error bars indicate SEM. Uptake is expressed as percentage of whole-body activity at 5 min after injection. (B) Abscess-to-background ratios determined by quantitative analysis of images of rabbits with *E. coli* infection injected with either ^{123}I -BH-IL-8 (●) or ^{123}I -iod-IL-8 (○). Error bars indicate SEM.

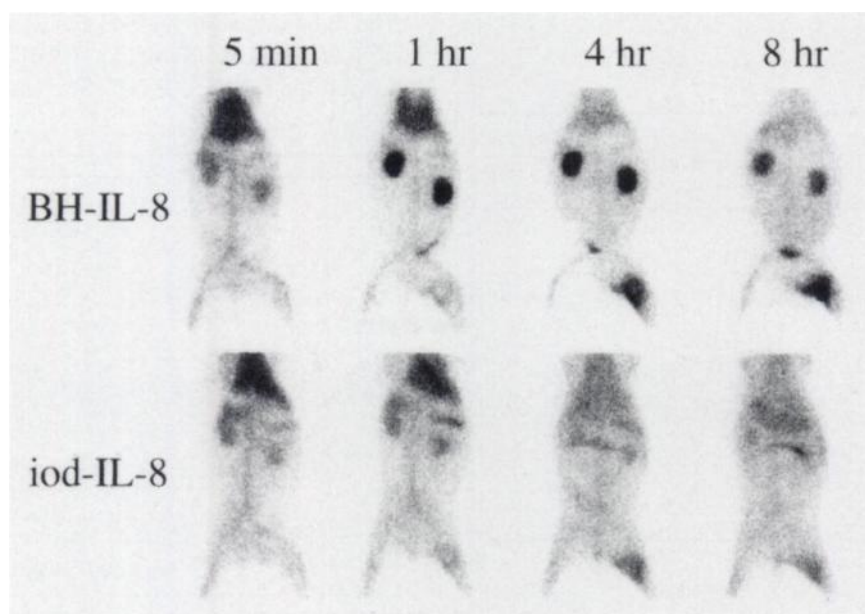


FIGURE 5. Images of rabbits with *E. coli* abscess in left thigh muscle at 5 min and at 1, 4, and 8 h after injection of either ^{123}I -BH-IL-8 (top row) or ^{123}I -iod-IL-8 (bottom row). All photographs were produced with same image contrast.

TABLE 1
Biodistribution of ^{123}I -BH-IL-8 and ^{123}I -Iod-IL-8 in Rabbits
with *E. coli* Infections at 8 Hours After Injection

Organ	%ID/g	
	^{123}I -BH-IL-8	^{123}I -Iod-IL-8
Blood	0.005 ± 0.0003	0.089 ± 0.020
Abscess	0.057 ± 0.011	0.119 ± 0.024
Muscle	0.0005 ± 0.00004	0.014 ± 0.003
Bone	0.002 ± 0.0003	0.028 ± 0.006
Marrow	0.026 ± 0.002	0.054 ± 0.009
Lung	0.039 ± 0.010	0.108 ± 0.016
Spleen	0.039 ± 0.010	0.080 ± 0.020
Kidney	0.066 ± 0.007	0.108 ± 0.024
Liver	0.014 ± 0.002	0.045 ± 0.020
Intestine	0.008 ± 0.0007	0.030 ± 0.00
Feces	0.008 ± 0.0006	0.011 ± 0.0002
Ratio		
Abscess-to-muscle	114.7 ± 23.0	8.3 ± 1.8
Abscess-to-blood	12.1 ± 2.2	1.4 ± 0.1

Data are expressed as mean \pm SEM.

the Bolton-Hunter method (^{123}I -BH-IL-8) was used. The blood levels of ^{123}I -Iod-IL-8 at 8 h after injection were significantly higher than those of ^{123}I -BH-IL-8 ($P < 0.0005$). Because of slower background clearance, the uptake of ^{123}I -Iod-IL-8 in all organs, including the abscess (Fig. 6A), was higher than that with ^{123}I -BH-IL-8. For most organs (i.e., abscess, noninfected muscle, bone, bone marrow, lung, and intestine including feces), these differences were significant ($P < 0.05$). These observations are clearly illustrated by the images (Fig. 5). The slow background clearance resulted in poor visualization of the abscesses with ^{123}I -Iod-IL-8 compared with clear delineation of the abscesses with ^{123}I -BH-IL-8. The abscess-to-background ratios of ^{123}I -BH-IL-8 were significantly higher than those of ^{123}I -Iod-IL-8 from 1 h after injection onward ($P < 0.01$) (Fig. 6B). Tissue biodistribution revealed an abscess-to-contralateral muscle ratio of ^{123}I -Iod-IL-8 of 8.3 ± 1.8 at 8 h after injection, which was significantly lower than that of ^{123}I -BH-IL-8 ($P < 0.05$) (Table 1). Furthermore, the abscess-to-blood ratio was also significantly lower for ^{123}I -Iod-IL-8 compared with that obtained with ^{123}I -BH-IL-8 ($P < 0.05$).

DISCUSSION

The potential of radiolabeled IL-8 for imaging infection and inflammation was investigated in a rabbit model of infection. High accumulation in the infection within a few hours after injection and rapid clearance from the background characterized the biodistribution of IL-8. These characteristics approximate the profile of an ideal radiopharmaceutical (22), making this protein very promising for clinical application.

The in vivo behavior of IL-8 labeled using the Bolton-Hunter method was more favorable than when the Iodo-Gen method was used. The clearance was much faster and the

abscess uptake was relatively higher, resulting in 10 times higher abscess-to-blood ratios and 14 times higher abscess-to-contralateral muscle ratios. The observed biodistribution of IL-8 labeled using the Iodo-Gen method was in line with results obtained by Hay et al. (23). They studied the in vivo behavior of IL-8 labeled using the chloramine-T method in rats with carrageenan-induced inflammation. Their quantitative imaging analysis revealed an abscess-to-background ratio of 2.5 from 1 h after injection onward, which was comparable to the ratios we obtained with IL-8 labeled using the Iodo-Gen method but much lower than the ratios obtained with IL-8 labeled using the Bolton-Hunter method. More rapid normal tissue clearance of proteins labeled with N-succinimide esters compared with those labeled using oxidative methods such as chloramine-T and Iodo-Gen has also been reported by Zalutsky and Narula (24) and Garg et al. (25). They have indicated that the difference in clearance was associated with differences in clearance of the low molecular weight catabolic products. The major catabolic product using N-succinimide esters containing a phenol group was benzoic acid, whereas iodide was the primary urinary catabolite when an oxidative method was used. Benzoic acids cleared considerably faster than did iodide, most likely because of formation of conjugates with glycine, which are rapidly excreted in the urine as hippuric acid (26). The binding of radiolabeled IL-8 to its receptors in the infectious tissue was not affected by the labeling method because similar in vitro receptor-binding capacities were found after radioiodination. In addition, it is unlikely that the processing of receptor-bound IL-8 was different because it has been shown that the processing of receptor-bound proteins labeled by the Bolton-Hunter method and the chloramine-T method is similar (27). Therefore, probably the observed differences in uptake of ^{123}I in the abscesses were associated with the differences in clearance of the catabolic products of both radiolabeled preparations.

Compared with other recently tested immunoproteins and peptides iodinated by the Bolton-Hunter method—i.e., IL-1, IL-1 receptor antagonist, and chemotactic peptides (28)—IL-8 displayed superior characteristics for infection imaging. The highest abscess uptake of IL-8, obtained after 4 h, was 2–5 times higher than the highest uptake of the other agents, obtained after 8 h, whereas the normal tissue clearance was similar. Abscess-to-background ratios of iodinated IL-8, as assessed by quantitative analysis of the images (highest value of 13 at 8 h after injection), were even 2 times higher than the ratios of $^{99\text{m}}\text{Tc}$ -labeled chemotactic peptides (highest value of 7 at 16–20 h after injection) (28–30). Moreover, the accumulation of $^{99\text{m}}\text{Tc}$ -labeled chemotactic peptides in liver, spleen, kidneys, and bowel may hamper detection of foci in the abdomen. In contrast, except for the kidneys, the tissue with the infection had the highest ^{123}I -IL-8 uptake as early as 8 h. The low background levels throughout the whole body, including the abdomen, would allow visualization of foci in almost any part of the body within the time span of several hours.

Immediately after injection, IL-8 induced transient leukopenia followed by leukocytosis. The leukopenia and leukocytosis were caused mainly by changes in granulocyte counts. Other systemically administered neutrophil chemotactic substances such as fMet-Leu-Phe-Lys and C5a induced neutropenia comparable with that observed for IL-8 (29,31). Furthermore, other investigators found similar neutropenia after intravenous injection of IL-8 in rabbits and nonhuman primates (32,33). The neutropenia was shown to be caused by cell stiffening, which results in transient trapping of activated neutrophils in capillaries (34), in particular in the microvessels of the lungs (32,35). Subsequent to the leukopenia, leukocytosis developed, which persisted more than 1 h after injection. Others have reported that the leukocytosis was present as long as IL-8 levels were detectable in the circulation (33,36). Possible mechanisms for the induction of leukocytosis by systemically administered IL-8 include recruitment of mature neutrophils from the marginal pool in the lung and other organs by inhibition of adhesion to the endothelium (36,37) and recruitment of immature neutrophils from the bone marrow by chemotactic properties of IL-8 (35,38). The rapid clearance and accumulation of ^{123}I -IL-8 mainly in the lungs, but also in the liver and spleen, observed within 10 min after injection, likely reflected receptor-bound ^{123}I -IL-8 on trapped neutrophils in the microcirculation of these organs. During the onset of the leukocytosis (i.e., 10–60 min after injection), a plateau in the blood clearance pattern of ^{123}I -IL-8, and sometimes even a rise in ^{123}I -IL-8 levels, was found. Release of neutrophils and ^{123}I -IL-8 from the lung and other organs seems to be the most plausible explanation for this phenomenon. Further clearance of ^{123}I -IL-8 was noticed after 30–60 min, probably caused by rapid dissociation and degradation of receptor-bound ^{123}I -IL-8 (39) and rapid clearance of circulating ^{123}I -IL-8 and its catabolites.

The high accumulation of ^{123}I -IL-8 in the abscess was most likely related to the high-affinity binding of IL-8 to its receptor on neutrophils. The interaction with the receptor may take place in the infectious tissue or, alternatively, in the circulation followed by migration of the neutrophils with receptor-bound IL-8 to the site of infection. The in vivo behavior of IL-8 must be examined in future experiments to elucidate the mechanism of accumulation at the site of infection.

The characteristics of IL-8 for imaging of infection are clearly superior to any of the receptor-binding agents that we have tested so far (28). However, a major drawback is the biologic activity of IL-8. The induced leukopenia by sequestration of neutrophils in the lungs and other organs and the subsequent leukocytosis were the main side effects that were noticed after systemic administration in mice, rabbits, and nonhuman primates (31,32,35). No hemodynamic changes were observed (32). These systemic side effects may present a problem with clinical application. Therefore, the aim of our current studies is to develop a radiolabeled IL-8 preparation with reduced biologic activity. Furthermore, for

clinical application, the expensive (^{123}I) and laborious labeling method (Bolton-Hunter) will not be preferable. Instead, efforts must be made to develop a simple and rapid labeling procedure using the radionuclide $^{99\text{m}}\text{Tc}$.

CONCLUSION

These studies show that ^{123}I -labeled IL-8 is an excellent agent to image infection: It rapidly accumulated in the infectious focus and rapidly cleared from nontarget tissues. The characteristics of IL-8 for imaging infection in this rabbit model are clearly superior to any of the receptor-binding agents that we have tested so far. These results warrant further development of an IL-8-based radiopharmaceutical for infection imaging that can be evaluated in clinical studies.

ACKNOWLEDGMENTS

The authors thank Peter Mast for determination of the leukocyte counts (University of Nijmegen, Department of Hematology) and Gerrie Grutters, Hennie Eijkholt, Bianca de Weem, and Geert Poelen (University of Nijmegen, Central Animal Laboratory) for technical assistance in the animal studies.

REFERENCES

1. Lavender JP, Lowe J, Barker JR, Burn JJ, Chaudri MA. Gallium-67 citrate scanning in neoplastic and inflammatory lesions. *Br J Radiol.* 1971;44:361–366.
2. McAfee JG, Gagne G, Subramanian G, Schneider RF. The localization of indium-111-leucocytes, gallium-67, polyclonal IgG and other radioactive agents in acute focal inflammatory lesions. *J Nucl Med.* 1991;32:2126–2131.
3. Oyen WJG, Claessens RAMJ, van der Meer JWM, Corstens FHM. Biodistribution and kinetics of radiolabelled proteins in rats with focal infection. *J Nucl Med.* 1992;33:388–394.
4. Babich JW, Graham W, Barrow SA, Fischman AJ. Comparison of the infection imaging properties of a $^{99\text{m}}\text{Tc}$ -labeled chemotactic peptide with ^{111}In IgG. *Nucl Med Biol.* 1995;22:643–648.
5. Babich JW, Graham W, Barrow SA, et al. Technetium-99m-labeled chemotactic peptides: comparison with indium-111-labeled white blood cells for localizing acute bacterial infection in the rabbit. *J Nucl Med.* 1993;34:2176–2181.
6. Van der Laken CJ, Boerman OC, Oyen WJG, et al. Specific targeting of infectious foci with radioiodinated human recombinant interleukin-1 in an experimental model. *Eur J Nucl Med.* 1995;22:1249–1255.
7. Van der Laken CJ, Boerman OC, Oyen WJG, et al. The behaviour of radiolabeled human recombinant interleukin-1 in various mouse inflammation models [abstract]. *Eur J Nucl Med.* 1996;23:1067P.
8. Chianelli M, Mather SJ, Procaccini EC, et al. In vivo detection of lymphocytic infiltration in thyroid autoimmune diseases by $^{99\text{m}}\text{Tc}$ -IL-2 [abstract]. *Eur J Nucl Med.* 1996;23:1055P.
9. Ben-Baruch A, Michiel DF, Oppenheim JJ. Signals and receptors involved in recruitment of inflammatory cells. *J Biol Chem.* 1995;270:11703–11706.
10. Yoshimura T, Matsushima K, Oppenheim JJ, Leonard EJ. Neutrophil chemotactic factor produced by lipopolysaccharide (LPS)-stimulated human blood mononuclear leukocytes: partial characterization and separation from interleukin-1 (IL-1). *J Immunol.* 1987;139:788–793.
11. Endo H, Akahoshi T, Takagishi K, Kashiwazaki S, Matsushima K. Elevation of interleukin-8 (IL-8) levels in joint fluids of patients with rheumatoid arthritis and the induction by IL-8 of leukocyte infiltration and synovitis in rabbit joints. *Lymphokine Cytokine Res.* 1991;10:245–252.
12. Miller EJ, Cohen AB, Nagao S, et al. Elevated levels of NAP-1/interleukin-8 are present in the airspaces of patients with the adult respiratory distress syndrome and are associated with increased mortality. *Am Rev Respir Dis.* 1992;146:427–432.
13. Mahida YR, Ceska M, Effenberger F, Kurlak L, Lindley I, Hawkey CJ. Enhanced synthesis of neutrophil-activating peptide-1/interleukin-8 in active ulcerative colitis. *Clin Sci (Colch).* 1992;82:273–275.

14. Izzo RS, Witkon K, Chen AI, Hadjiyane C, Weinstein MI, Pellechia C. Interleukin-8 and neutrophil markers in colonic mucosa from patients with ulcerative colitis. *Am J Gastroenterol*. 1992;87:1447-1452.
15. Holmes WE, Lee J, Kuang WJ, Rice GC, Wood WI. Structure and functional expression of a human interleukin-8 receptor. *Science*. 1991;253:1278-1280.
16. Murphy PM, Tiffany HL. Cloning of complementary DNA encoding a functional human interleukin-8 receptor. *Science*. 1991;253:1280-1283.
17. Lee J, Horuk R, Rice GC, Bennett GL, Camerato T, Wood WI. Characterization of two high affinity human interleukin-8 receptors. *J Biol Chem*. 1992;267:16283-16287.
18. Cerretti DP, Kozlosky CJ, VandenBos T, Nelson N, Gearing DP, Beckmann MP. Molecular characterization of receptors for human interleukin-8, GRO/melanoma growth-stimulatory activity and neutrophil activating peptide-2. *Mol Immunol*. 1993;30:359-367.
19. Wilbur DS, Hadley SW, Hylarides MD, et al. Development of a stable radioiodinating reagent to label monoclonal antibodies for radiotherapy of cancer. *J Nucl Med*. 1989;30:216-226.
20. Fraker PJ, Speck JC. Protein and cell membrane iodination with a sparingly soluble chloramide 1,3,4,6-tetrachloro-3 α ,6 α -diphenyl-glucouril. *Biochem Biophys Res Commun*. 1978;80:849-857.
21. Lindmo T, Boven E, Cuttita F, Fedorko J, Bunn PA. Determination of the immunoreactive fraction of radiolabeled monoclonal antibodies by linear extrapolation to binding at infinite cell excess. *J Immunol Method*. 1984;72:77-89.
22. Corstens FHM, van der Meer JWM. Chemotactic peptides: new locomotion for imaging of infection? *J Nucl Med*. 1991;32:491-494.
23. Hay RV, Skinner RS, Newman OC, et al. Nuclear imaging of acute inflammatory lesions with recombinant human interleukin-8 [abstract]. *J Nucl Med*. 1993;34:104P.
24. Zalutsky MR, Narula AS. Radiohalogenation of a monoclonal antibody using an N-succinimidyl 3-(tri-n-butylstannyl)benzoate intermediate. *Cancer Res*. 1988;48:1446-1450.
25. Garg PK, Alston KL, Zalutsky MR. Catabolism of radioiodinated murine monoclonal antibody F(ab')₂ fragment labeled using N-succinimidyl 3-iodobenzoate and Iodogen methods. *Bioconjug Chem*. 1995;6:493-501.
26. Goodman LS, Gilman A. *The Pharmacological Basis of Therapeutics*. New York, NY: Macmillan; 1975:994.
27. Shih LB, Thorpe SR, Griffiths GL, et al. The processing and fate of antibodies and their radiolabels bound to the surface of tumor cells in vitro: a comparison of nine radiolabels. *J Nucl Med*. 1994;35:899-908.
28. van der Laken CJ, Boerman OC, Oyen WJG, van de Ven MTP, van der Meer JWM, Corstens FHM. Comparison of potential of interleukin-1, its receptor antagonist and a chemotactic peptide for imaging of infection: a comparative study. *Eur J Nucl Med*. 1998;25:347-352.
29. van der Laken CJ, Boerman OC, Oyen WJG, et al. Tc-99m-labeled chemotactic peptides specifically localize in acute infection and sterile inflammation. *J Nucl Med*. 1997;38:1310-1315.
30. Babich JW, Graham W, Barrow SA, et al. Technetium-99m-labeled chemotactic peptides: comparison with indium-111-labeled white blood cells for localizing acute bacterial infection in the rabbit. *J Nucl Med*. 1993;34:2176-2181.
31. Kajita T, Hugli TE. C5a-induced neutrophilia: a primary humoral mechanism for recruitment of neutrophils. *Am J Pathol*. 1990;137:467-477.
32. Hechtman DH, Cybulsky MI, Fuchs HJ, Baker JB, Gimbrone MA Jr. Intravascular IL-8: inhibitor of polymorphonuclear leukocyte accumulation at sites of acute inflammation. *J Immunol*. 1991;147:883-892.
33. Van Zee KJ, Fischer E, Hawes AS, et al. Effects of intravenous IL-8 administration in nonhuman primates. *J Immunol*. 1992;148:1746-1752.
34. Worthen GS, Schwab B III, Elson EL, Downey GP. Mechanics of stimulated neutrophils: cell stiffening induces retention in capillaries. *Science*. 1989;245:183-186.
35. Laterveer L, Lindley IJD, Heemskerk DPM, et al. Rapid mobilization of hematopoietic progenitor cells in Rhesus monkeys by a single intravenous injection of interleukin-8. *Blood*. 1996;87:781-788.
36. Simonet WS, Hughes TM, Nguyen HQ, Trebasky LD, Danilenko DM, Medlock ES. Long-term impaired neutrophil migration in mice overexpressing human interleukin-8. *J Clin Invest*. 1994;94:1310-1319.
37. Westlin WF, Kiely JM, Gimbrone MA. Interleukin-8 induces changes in human neutrophil actin conformation and distribution: relationship to inhibition of adhesion to cytokine-activated endothelium. *J Leukoc Biol*. 1992;52:43-51.
38. Van Damme J, Van Beeumen J, Opendakker G, Billiau A. A novel NH₂-terminal sequence-characterized human monokine possessing neutrophil chemotactic, skin-reactive and granulocytosis-promoting activity. *J Exp Med*. 1988;167:1364-1376.
39. Besemer J, Hujber A, Kuhn B. Specific binding, internalization, and degradation of human neutrophil activating factor by human polymorphonuclear leukocytes. *J Biol Chem*. 1989;264:17409-17415.